American Mineralogist, Volume 74, pages 5–13, 1989

Dependence of entropy on volume for silicate and oxide minerals: A review and a predictive model

TIMOTHY J. B. HOLLAND
Department of Earth Sciences, University of Cambridge, Downing Street, Cambridge CB2 3EQ, England

ABSTRACT

Simple quantum models (Einstein and Debye) of lattice heat capacity and entropy may be used to predict the magnitude of the dependence of entropy on volume for silicate minerals. The origins for the volume effect as well as the effect of variation in coordination state of cation polyhedra on the third-law entropy are explored and rationalized within the framework of simple lattice-vibration theory. It is shown that Einstein and Debye theories for solids predict a value for $(\partial S/\partial V)_{298}$ of about 1.0 $J \cdot K^{-1} \cdot cm^{-3}$, precisely the value found from regression of a set of 60 experimentally measured entropies and volumes of silicates and oxides. An additive model for estimating the entropies of mineral end-members at 298 K, based upon the scheme advocated by Fyfe, Turner, and Verhoogen (1958), but allowing for coordination changes, is developed and evaluated by multiple regression of this body of measured data. The entropy-volume-coordination model fits these data better than any previously published scheme and works remarkably well even for transition metal–bearing phases when allowance for magnetic disordering is made. Phases such as magnetite and hematite that undergo magnetic disorder at temperatures above 298 K can be accommodated within the model by correcting for the partial disorder at 298 K using simple Landau theory. The model predicts silicate and oxide entropies in the system K_2O-Na_2O-CaO-MgO-FeO-Fe_2O_3-MnO-TiO_2-Al_2O_3-SiO_2 with uncertainties typically in the range of 0–2%, even for the Fe-, Mn-, and Ti-bearing phases.

INTRODUCTION

As increasing reliance is being placed on thermodynamic modeling to interpolate and extrapolate experimentally determined mineral equilibria in petrology, so the need for reliable estimates of entropy for mineral phases increases accordingly. While recent years have seen a remarkable number of new precise experimental determinations of the heat capacities and, by direct integration, the entropies of mineral end-members, there are still many phases remaining that require methods of estimation. The reasons for this need, which will never entirely disappear, are (1) calorimetric determinations of entropy require considerable effort and are time-consuming; (2) often a chosen mineral end-member cannot easily be obtained either in pure enough form or in sufficient quantity for measurement; or (3) the end-members to be determined are fictive in the sense that they are not stable for the chosen structure or composition.

In principle at least, entropies (and all other thermodynamic functions) may be calculated from spectroscopic determination of the lattice-vibration spectrum for solid crystalline materials. Rigorous determinations have rarely been attempted (but see Salje and Werneke, 1982, for andalusite and sillimanite) although simplifications in modeling the phonon density of states function, as in Kieffer (1980), have produced encouraging results. Apart from the fact that this approach is even more labor-intensive than direct calorimetry and therefore unlikely to become commonly used, there still remains the problem of unavailability of the required material in pure form or in the relevant structural state. The astonishing success of Price et al. (1987) in accurately predicting the heat capacity, entropy, and compressibility of forsterite from a set of independently derived interionic potentials holds obvious promise for the future—if this technique becomes widely used (and extended to a larger system than Mg-Si-O). However, until such time, simpler, quicker methods must be found that afford reliable estimates of mineral entropies and that can be based on a minimum of measured properties.

Past efforts to find estimates of entropy have been remarkably successful at the 5–15% accuracy level, and all involve some modification of the Newmann-Kopp rule, which is based on the observation that heat capacities (and therefore entropies) of complex compounds may be estimated by summing, in stoichiometric proportions, the heat capacities or entropies of simpler chemical entities. Latimer (1951, 1952) and Fyfe et al. (1958) used entropies of the elements and of oxides respectively to estimate entropies of more complex compounds. Fyfe et al. noted the positive correlation between molar volume and entropy and incorporated a simple volume correction factor in their estimation scheme:

$$S_j = \Sigma n_i S_i + k(V_j - \Sigma n_i V_i),$$

0003–004X/89/0102–0005$02.00

where S_j is the entropy (to be determined) of phase j, V_j is the molar volume of phase j, whereas S_i and V_i are entropies and volumes of the n_i oxide components i required to make up phase j, and k is an arbitrary constant determined from measurements.

Helgeson et al. (1978) improved matters somewhat by taking structurally analogous mineral phases as components instead of oxides; this has the advantage that differences in coordination state between the components and the phase "being built" are minimized. It has long been recognized that the coordination state affects the entropy; the difference between Al in octahedral and tetrahedral sites may be readily evaluated and has been used in simple calculations (e.g., Holland and Richardson, 1979) on mineral stability. Recognizing the importance of coordination, Robinson and Haas (1983) used multiple regression to derive a set of fictive oxide components from the available measured mineral entropies and heat capacities. The result was a set of oxide components, in varying coordination states, which could be summed directly to estimate the entropy of any desired oxide or silicate. While having the advantage over the structural analogue approach of path independence, the neglect in Robinson and Haas's model of the volume correlation, which was so successful in earlier approaches, makes their method less powerful than it could have been.

It was the lack of TiO_2, MnO, and Fe_2O_3 in the Robinson and Haas scheme as well as its inability to predict accurate entropies for common pyroxene and amphibole components that led to the model proposed here. Some of the more notable entropy discrepancies in the Robinson and Haas method (see column RH in Table 2) are hercynite ($+11$ J·K^{-1}), cordierite ($+17$ J·K^{-1}), jadeite (-16 J·K^{-1}), tremolite (-21 J·K^{-1}), leucite ($+12$ J·K^{-1}), pyrope (-14 J·K^{-1}) and grossular ($+43$ J·K^{-1}), all of which would cause unacceptable errors in phase-equilibrium calculations. The volume-corrected methods of Fyfe et al. (1958) and Helgeson et al. (1978) generally work quite well, and there are sound theoretical reasons for a positive correlation between volume and entropy that warrant a brief review before presenting the revised estimation method and results.

The entropy-volume relationship reviewed

Although the relationship of entropy to mass is well known and has been discussed and used by Latimer (1951, 1952), in the methods to be discussed below, fictive components are summed to "build" mineral entropy so that mass is conserved. In their discussions, Fyfe et al. (1958) called upon the relation

$$(\partial S/\partial V)_T = \alpha/\beta = (\partial P/\partial T)_V$$

to explain the positive correlation of entropy with volume and to justify the positive sign of the correlation. While it is true that α/β, the ratio of thermal expansion to compressibility, is generally a small positive number, this equation does not provide a satisfying explanation of the effect at an atomistic or structural level. The reason for a positive correlation of entropy with volume can be seen most easily by considering the role of lattice vibrations in determining the heat capacities and entropies of crystalline solids. The simplest quantum model for lattice heat capacity was devised by Einstein to explain the fall off of heat capacity to zero as the absolute zero of temperature is approached. In this model the crystal is assumed to be composed of $3N$ independent one-dimensional harmonic oscillators vibrating with frequency ν, where N is Avogadro's number. The Einstein model heat capcity for 1 mol of a phase containing n atoms in its formula unit is given by

$$C_V = 3nR[u^2e^u/(e^u - 1)^2],$$

where R is the gas constant, and $u = h\nu/kT$, with h and k being Planck's constant and Boltzmann's constant, respectively. The entropy according to this model is

$$S = 3nR\{[u/(e^u - 1)] - \ln(1 - e^{-u})\}.$$

While the heat capacity of an Einstein crystal does not match the behavior of real crystals perfectly at low temperatures, it does simulate the trend remarkably well for a simple one-parameter model.

Next to be considered is the role of molar volume, whose importance lies in its relationship to the term $u = h\nu/kT$. Enlarging the cell volume of a simple crystal whose atoms vibrate at a characteristic frequency has the effect of moving apart the component atoms, thus reducing their bond stiffnesses and lowering their vibrational frequency (in proportion to $(V_0/V)^{1/3}$). Figure 1 illustrates the general dependence of heat capacity on vibrational frequency, and from the definition of the third-law entropy,

$$S_T = \int_0^T \frac{C_P}{T}\,dT,$$

one can see clearly that lowering the frequency by lengthening and weakening the bonds causes an increase in entropy. To be more rigorous, C_P must be converted to C_V with the relation

$$C_P = C_V + TV\alpha^2/\beta,$$

although the difference is negligible at low temperatures for solids.

The magnitude of the volume effect on the entropy of an Einstein solid is given by

$$(\partial S/\partial V)_{298} = (\partial u/\partial V)(\partial S/\partial u)_{298}$$

which, from $u = u_0(V_0/V)^{1/3}$ and the Einstein expression above for the entropy, one finds by substitution that

$$(\partial S/\partial V)_{298} = nRu^2/[V(e^u - 1)(1 - e^{-u})].$$

In this expression, V is the molar volume of the mineral concerned. Evaluating this expression at 298 K for all phases listed in Table 1, the mean value of $(\partial S/\partial V)_{298}$ is found to be 1.07 ± 0.11 J·K^{-1}·cm^{-3}. This value is a numerical measure of the constant k in the Fyfe et al. en-

tropy-estimation scheme discussed above and is in excellent agreement with the value found empirically below.

Although the above model is simple, the Einstein approximation is nevertheless remarkable in describing, with only one adjustable parameter, the heat capacity and entropy of crystals, and it should give a reliable estimate of the volume dependence of the entropy. The relationship of normal mode frequencies to entropy will be explored further later, but in passing it should be noted that the effect of volume on heat capacity will lessen at higher temperature where thermal agitation is more pronounced and will tend to mask the smaller volume-related effect. It is for this reason that high-temperature heat capacities may be modeled quite reasonably by a simple additivity of oxides approach without consideration of the volume correction (as done by Berman and Brown, 1985).

It is interesting to inquire whether an increase in the sophistication of the assumptions used alters this result, and so the above exercise was repeated using the Debye model for heat capacities. In place of a single frequency to characterize the vibrational spectrum, Debye assumed a quadratic density of states $g(\nu) = a\nu^2$, which is the correct behavior in the low-frequency limit for a continuum, with a cut-off value at ν_{max}. A similar approach to that taken above, using the Debye (D) expression for the entropy with $\theta_D = h\nu_{max}/k$ expressed in parameterized form, gives

$$S_{298,D} = n(13141/\theta_D - 3.81)$$

where the constants were determined from a least-squares fit to the Debye entropy function at 298 K and entropy is in $J \cdot K^{-1} \cdot mol^{-1}$; hence,

$$(\partial S/\partial V)_{298} = (S + 3.81n)/3V,$$

which on evaluation (Table 1) gives a slightly lower value of $(\partial S/\partial V)_{298} = 0.93 \pm 0.10\ J \cdot K^{-1} \cdot cm^{-3}$. Given that the Debye approximation is often used best in the low-temperature limit and the Einstein model often works well for approximating the high-temperature behavior, an average might be appropriate, and a value of unity for the proportionality constant k is accepted, as predicted from simple lattice-vibration models.

The relationship between entropy and coordination

Having examined the entropy-volume relationship, I now turn to look briefly at the role of coordination state. As a simple example, I will take the Ca_2SiO_4 minerals larnite and calcium olivine that have entropy values of 127.6 $J \cdot K^{-1}$ and 120.5 $J \cdot K^{-1}$, respectively, despite larnite having the smaller volume. Clearly larnite owes its higher entropy to the distorted and much larger site for one of its two Ca ions (see Table 1), while presumably it manages to keep its volume reduced by a suitable packing arrangement of alternating large (M2) and small (M1) Ca sites. Thus the dominant control of the entropy difference between Ca olivine and larnite lies in the coordination change from 6 to 8 one of its Ca sites, as would be predicted by the simple vibrational models discussed above. Kieffer (1982) has drawn attention to the fact that the entropy is sensitive to the position of the lowest-frequency optic modes, which are those usually associated with internal vibrational modes of cation polyhedra in silicates, and one should thus expect, as a general rule, that increasing coordination state will lead to an increase in entropy.

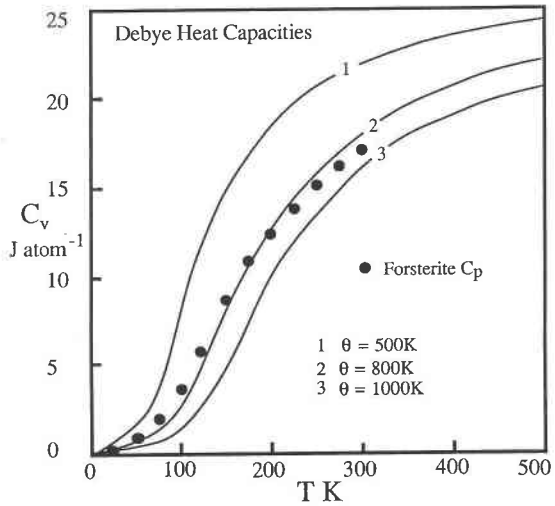

Fig. 1. Heat capacities calculated from the Debye theory using three values for the Debye temperature θ_D to show the effect of varying the vibrational frequency ($\theta_D = h\nu/k$). Filled circles are experimentally measured C_P data for forsterite.

Exceptions to this simple notion are numerous, and it is often impossible to apply it straightforwardly to complex silicates because in many instances it is not the internal modes associated with a coordination polyhedron that dominate the low-temperature heat capacity, but the external modes associated with the linkages between the polyhedra. A classic example is the case of the three aluminosilicate polymorphs kyanite, andalusite, and sillimanite. All three minerals contain SiO_4 tetrahedra and chains of edge-connected AlO_6 octahedra, but an extra Al in the formula occurs in 6-fold octahedra in kyanite, in irregular 5-fold coordinated polyhedra in andalusite, and in 4-fold tetrahedra in sillimanite. The entropies at 298 K are 82.3, 91.4, and 95.8 $J \cdot K^{-1} \cdot mol^{-1}$, respectively; thus it is usually argued that the entropy increase in these minerals occurs in response to reduction in the coordination state. However, in these polymorphs the entropies increase in the reverse order from that predicted by the frequencies of the internal vibrational modes; the average polyhedral Al–O bond is shortest and stiffest in the tetrahedral sites (sillimanite) and longest in the octahedral sites (as in kyanite), yet Kieffer (1982) noted that the lowest-frequency optic mode occurs at 115 cm^{-1} in sillimanite, at 156 cm^{-1} in andalusite, and at 237 cm^{-1} in kyanite. Thus it is reasonable to infer that it is not the internal vibrational modes of the characteristic Al polyhedra in these silicates that dominate the sequence of lowest optic

TABLE 1. Entropy, volume, and composition data for phases used in the regression

Phase*	V**	S†	Ref.§	Phase*	V**	S†	Ref.§
Magnetite (mt) Fe_2O_3, FeO	44.53	126.2 (−19.9)‡	1	Wollastonite (wo) $^{[6]}CaO$, SiO_2	39.93	81.7	10
Hematite (hem) Fe_2O_3	30.27	82.3 (−5.1)‡	1	Calcium Tschermak's pyroxene (cats) $^{[8]}CaO$, $0.5^{[6]}Al_2O_3$, $0.5^{[4]}Al_2O_3$, $^{[4]}SiO_2$	63.56	135.3	11
Titanomagnetite (Timt) 2FeO, $^{[6]}TiO_2$	46.82	142.1 (−26.8)‡	1	Diopside (di) $^{[8]}CaO$, $^{[6]}MgO$, $2^{[4]}SiO_2$	66.19	142.7	10
Calcium ferrite (CaFt) $^{[8]}CaO$, Fe_2O_3	44.98	115.6 (−29.8)‡	1	Enstatite (en) $^{[7]}MgO$, $^{[6]}MgO$, $2^{[4]}SiO_2$	62.68	132.5	10
Dicalcium ferrite (DCFt) $2^{[6]}CaO$, Fe_2O_3	67.18	159.0 (−29.8)‡	1	Rhodonite (rho) $^{[6]}MnO$, $^{[4]}SiO_2$	35.16	87.6 (−14.9)‡	1
Acmite (acm) $0.5^{[8]}Na_2O$, $0.5Fe_2O_3$, $2^{[4]}SiO_2$	64.59	155.7 (−14.9)‡	2	Tremolite (tr) $2^{[8]}CaO$, $5^{[6]}MgO$, $8^{[4]}SiO_2$, H_2O(b)	272.70	549.1	1
Jadeite (jd) $0.5^{[8]}Na_2O$, $0.5^{[6]}Al_2O_3$, $2^{[4]}SiO_2$	60.40	133.5	1	Anorthite (an) $^{[9]}CaO$, $^{[4]}Al_2O_3$, $2^{[4]}SiO_2$	100.79	199.3	1
Ilmenite (ilm) FeO, $^{[6]}TiO_2$	31.69	95.5 (−13.4)‡	1, 3	Merwinite (merw) $3^{[9]}CaO$, $^{[6]}MgO$, $2^{[4]}SiO_2$	98.47	253.1	1
Spinel (sp) $^{[4]}MgO$, $^{[6]}Al_2O_3$	39.78	80.6	1	Microcline (micr) $0.5^{[a]}K_2O$, $0.5^{[4]}Al_2O_3$, $3^{[4]}SiO_2$	108.72	214.2	1
Rutile (ru) $^{[6]}TiO_2$	18.82	50.3	1	Kaliophilite (kal) $0.5^{[a]}K_2O$, $0.5^{[4]}Al_2O_3$, $^{[4]}SiO_2$	59.89	133.3	1
Tridymite (trid) $^{[4]}SiO_2$	26.53	43.9	1	Leucite (lc) $0.5^{[b]}K_2O$, $0.5^{[4]}Al_2O_3$, $2^{[4]}SiO_2$	88.39	184.3	1
Manganosite (mang) $^{[6]}MnO$	13.22	44.8 (−14.9)‡	1	Albite (ab) $0.5^{[9]}Na_2O$, $0.5^{[4]}Al_2O_3$, $3^{[4]}SiO_2$	100.04	207.4	1
Lime (lime) $^{[6]}CaO$	16.76	38.1	1	Nepheline (ne) $0.5^{[9]}Na_2O$, $0.5^{[4]}Al_2O_3$, $^{[4]}SiO_2$	54.16	124.4	1
Periclase (per) $^{[6]}MgO$	11.25	27.0	1	Muscovite (mu) $0.5^{[b]}K_2O$, $^{[6]}Al_2O_3$, $0.5^{[4]}Al_2O_3$, $3^{[4]}SiO_2$, H_2O(a)	140.83	287.7	1
Corundum (cor) $^{[6]}Al_2O_3$	25.58	50.9	1	Phlogopite (ph) $0.5^{[b]}K_2O$, $3^{[6]}MgO$, $0.5^{[4]}Al_2O_3$, $3^{[4]}SiO_2$, H_2O(b)	149.64	315.9	12
Hercynite (herc) FeO, $^{[6]}Al_2O_3$	40.75	92.9 (−13.4)‡	1	Talc (ta) $3^{[6]}MgO$, $4^{[4]}SiO_2$, H_2O(b)	136.25	260.8	1
Hedenbergite (hed) $^{[8]}CaO$, FeO, $2^{[4]}SiO_2$	67.88	160.8 (−13.4)‡	4	Pyrophyllite (pph) $^{[6]}Al_2O_3$, $4^{[4]}SiO_2$, H_2O(a)	127.61	239.4	1
Ferrosilite (fs) 2FeO, $^{[4]}SiO_2$	65.92	162.5 (−26.8)‡	5	Anthophyllite (anth) $2^{[7]}MgO$, $5^{[6]}MgO$, $8^{[4]}SiO_2$, H_2O(b)	265.4	537.0	10
Kyanite (ky) $^{[6]}Al_2O_3$, $^{[4]}SiO_2$	44.09	82.3	6	Clinochlore (clin) $5^{[8]}MgO$, $0.5^{[6]}Al_2O_3$, $0.5^{[4]}Al_2O_3$, $3^{[4]}SiO_2$, $4H_2O$(b)	210.9	397.6	13
Sillimanite (sill) $0.5^{[6]}Al_2O_3$, $0.5^{[4]}Al_2O_3$, $^{[4]}SiO_2$	50.03	95.8	6	Margarite (ma) $^{[9]}CaO$, $^{[6]}Al_2O_3$, $^{[4]}Al_2O_3$, $2^{[4]}SiO_2$, H_2O(a)	129.60	263.6	14
Calcium olivine (caol) $2^{[6]}CaO$, $^{[4]}SiO_2$	59.11	120.5	1	Paragonite (pa) $0.5^{[9]}Na_2O$, $^{[6]}Al_2O_3$, $0.5^{[4]}Al_2O_3$, $3^{[4]}SiO_2$, H_2O(a)	132.11	277.1	12
Larnite (larn) $^{[6]}CaO$, $^{[8]}CaO$, $^{[4]}SiO_2$	51.6	127.6	1	Diaspore (dia) $0.5^{[6]}Al_2O_3$, $0.5H_2O$(a)	17.76	35.3	1
Gehlenite (geh) $^{[9]}CaO$, $^{[8]}CaO$, $^{[4]}Al_2O_3$, $^{[4]}SiO_2$	90.24	198.6	1	Gibbsite (gib) $0.5^{[6]}Al_2O_3$, $1.5H_2O$(a)	32.03	68.4	1
Akermanite (ak) $^{[8]}CaO$, $^{[9]}CaO$, $^{[4]}MgO$, $2^{[4]}SiO_2$	92.54	209.2	1	Prehnite (pre) $2^{[9]}CaO$, $0.5^{[6]}Al_2O_3$, $0.5^{[4]}Al_2O_3$, $3SiO_2$, H_2O(b)	140.26	292.8	14
Monticellite (mont) $^{[6]}CaO$, $^{[6]}MgO$, $^{[4]}SiO_2$	51.48	108.1	7	Chrysotile (chy) $3^{[6]}MgO$, $2^{[4]}SiO_2$, $2H_2O$(a)	107.46	221.3	1
Sphene (sph) $^{[8]}CaO$, $^{[6]}TiO_2$, $^{[4]}SiO_2$	55.65	129.3	1	Zoisite (zo) $2^{[9]}CaO$, $1.5^{[6]}Al_2O_3$, $3^{[4]}SiO_2$, $0.5H_2O$(b)	135.88	295.9	14
Fayalite (fa) 2FeO, $^{[4]}SiO_2$	46.30	124.2 (−26.8)‡	8	Almandine (alm) $3^{[8]}FeO$, $^{[6]}Al_2O_3$, $3SiO_2$	115.11	299.6 (−40.1)‡	15
Forsterite (fo) $2^{[6]}MgO$, $^{[4]}SiO_2$	43.66	94.1	9	Pyrope (py) $3^{[8]}MgO$, $^{[6]}Al_2O_3$, $3SiO_2$	113.18	266.3	16
Cordierite (crd) $2^{[6]}MgO$, $2^{[4]}Al_2O_3$, $5^{[4]}SiO_2$	233.22	407.1	1	Grossular (gr) $3^{[8]}CaO$, $^{[6]}Al_2O_3$, $3SiO_2$	125.35	254.7	17
Tephroite (teph) $2^{[6]}MnO$, $^{[4]}SiO_2$	48.61	133.4 (−29.8)‡	1	Andradite (andr) $3^{[8]}CaO$, $^{[6]}Fe_2O_3$, $3SiO_2$	132.04	286.6 (−29.8)‡	18

* Phase name, abbreviation, and composition. Numbers in brackets represent coordination state (see text).

** V, volume, in $cm^3 \cdot mol^{-1}$.

† S, entropy, in $J \cdot K^{-1} \cdot mol^{-1}$.

‡ Entropy corrected by this amount for magnetic and/or other disorder (see text).

§ References: (1) Robie et al., 1979; (2) Ko et al., 1977; (3) Anovitz et al., 1985; (4) Haselton et al., 1987; (5) Bohlen et al., 1983; (6) Robie and Hemingway, 1984a; (7) Sharp et al., 1986; (8) Robie et al., 1982a; (9) Robie et al., 1982b; (10) Krupka et al., 1985; (11) Haselton et al., 1984; (12) Robie and Hemingway, 1984b; (13) Henderson et al., 1983; (14) Perkins et al., 1980; (15) Bohlen et al., 1986; (16) Haselton and Westrum, 1980; (17) Perkins et al., 1977; (18) Robie et al., 1987.

modes, and hence entropies, but some unspecified external modes associated with the linking of the polyhedral units. We must therefore expect the common occurrence of phases in which the positive entropic effect of smaller and more rigid polyhedra is offset by the lower rigidity of the interconnecting framework. Given that the entropy and other thermodynamic properties are functions of the average vibrational spectrum, we might expect that the molar volume should reflect the overall bonding, and hence vibrational, state of the crystal. In the aluminosil-

icate example, the entropies of the three polymorphs are indeed proportional to their molar volumes.

From the above discussion it is clear that the effects of cation coordination as well as the volume contribution must be incorporated into the additivity models for mineral entropy estimation, although in many complex silicates it may be impossible to ascribe anomalous entropy to any one particular structural feature. Any model based solely on the coordination state and molar volume can form only a crude guide to the vibrational spectrum, but as shown below may be sufficiently accurate in predicting entropies of silicates from a minimum of information.

Some non-lattice-vibrational contributions to entropy

Contributions to the entropy arising from phenomena other than lattice-vibration effects have been discussed in considerable detail in the literature, and the interested reader may turn to the review article by Ulbrich and Waldbaum (1976) for more detail. For the present purposes, all such contributions to the 298-K entropy must be removed before looking at the relationship of entropy with volume, and so terms arising from magnetic as well as site disordering and possible electronic effects arising from Jahn-Teller site distortions and other crystal-field effects must be taken into account.

The site–configurational entropy terms involved in, for example, Al-Si order-disorder on tetrahedral sites, have been removed from the tabulated entropies, and only the calorimetric entropies have been used in the following analysis. Care must be taken when using tabulated entropies; in the tables of Robie et al. (1979), certain phases have had an arbitrary configurational term added, an example being muscovite for which the full $-4R[0.75 \ln(0.75) + 0.25 \ln(0.25)]$, amounting to 18.7 $J \cdot K^{-1} \cdot mol^{-1}$, has been added. It remains a debatable point whether this is always justified, and in the case of muscovite, the experimental phase relations are consistent only with a largely ordered state. Strong short-range order can reduce the entropy contribution to very small values, and recent work suggests that (Al,Si) in muscovite is ordered on a local basis (Herrero et al., 1987).

Magnetic order-disorder transformations at low temperatures are quite common in minerals containing transition metals and give rise to substantial heat-capacity anomalies (λ peaks) that contribute to the entropy at 298 K. Although the λ anomaly occurs at different temperatures and varies in size in different minerals, the contribution to the entropy is ideally given by $S = R \ln(2s + 1)$, where s is the spin quantum number. Thus, for Fe^{2+}, s is 2 and contributes $R \ln 5$ (13.4 $J \cdot K^{-1} \cdot atom^{-1}$), whereas for Fe^{3+} and Mn^{2+}, s is 5/2 and so the entropy contribution becomes $R \ln 6$ (14.9 $J \cdot K^{-1} \cdot atom^{-1}$). In the analysis to follow, these ideal entropies for magnetic disorder have been subtracted from the phases that have a low-temperature magnetic transformation. The minerals hematite and magnetite require special comment as they are characterized by having their magnetic λ transitions at temperatures well above 298 K, but have long tails to their λ anomalies extending down to temperatures below 298 K; thus there is likely to be some small contribution to the entropy arising from the incipient disorder of the magnetic spins below 298 K. One way of estimating the magnitude of this contribution is to apply simple Landau theory (for a good mineralogical review of the basic concepts, see Carpenter, 1988) to these magnetic transformations. Landau theory for tricritical behavior leads to the following useful expression for the entropy as a function of temperature below T_c:

$$S_{\text{Landau}} = S_{\max}[1 - (1 - T/T_c)^{1/2}]$$

where $S_{\max}$ is the maximum entropy expected for the transformation, i.e.,

$$S_{\max} = \int_0^{T_c} \frac{C_P^{\text{ex}}}{T} dT$$

and C_P^{ex} is the excess heat capacity relative to the fully ordered phase. It is conventional, in Landau theory, to take excess properties relative to the disordered, high-symmetry, phase, whereas the above expressions have been rearranged according to the more usual petrological convention. For hematite (T_c = 955 K, $S_{\max} = 2R \ln 6$), the entropy contribution at 298 K, from the equation above, is 5.1 $J \cdot K^{-1} \cdot mol^{-1}$, amounting to 17% of the maximum entropy that would be gained only at T = 955 K. The conclusion is that even though 298 K is well below T_c, the effect of the tail in the λ heat-capacity anomaly is not negligible, and the value of 5.1 $J \cdot K^{-1} \cdot mol^{-1}$ should be subtracted from the calorimetric entropy of hematite if one wishes to determine the lattice-vibrational portion of the entropy. A similar argument for magnetite (T_c = 848 K) suggests that the entropy of magnetite should be decremented by 8.4 $J \cdot K^{-1} \cdot mol^{-1}$ to allow for the λ tail effect. Magnetite still requires a further adjustment of approximately $-2R \ln 2$ $J \cdot K^{-1} \cdot mol^{-1}$ to allow for the disordering transformation (normal to inverse spinel) that occurs at 115 K.

A further problem is the variable entropy contribution from transition-metal ions (in this study in FeO, Fe_2O_3, TiO_2) due to polyhedral site distortions. The subject has been discussed by Wood (1981) who showed that crystal-field effects can be large and important for these cations under some circumstances. The effects discussed by Wood should be maximal only at very low temperatures and for extreme differences in the shape of a distorted and undistorted polyhedron; the success of the simple model to be discussed in the next section implies that at 298 K these crystal-field terms probably make only a small contribution to the entropy.

Proposed estimation method and results

Realizing the need to incorporate the effects of both volume and coordination and the fact that both of these are only an approximate guide to the vibrational contribution to the specific heat and entropy, one opts for the simplest possible model—that of Fyfe et al. (1958)—but allows some components to be represented in several dif-

TABLE 2. Results of regression for $S - V$ of phases

Phase*	hat	$S-V$ meas.	$S-V$ calc.	resid.	RH	k_D	k_E
mt	0.314	81.70	81.02	0.68	—	1.14	1.28
hem	0.283	52.03	50.24	1.79	—	1.12	1.26
Timt	0.364	95.29	94.18	1.11	—	1.20	1.33
CaFt	0.249	70.58	72.18	−1.60	—	1.05	1.19
DCFt	0.358	91.81	94.13	−2.32	—	0.96	1.08
acm	0.351	91.08	88.18	2.90	—	0.92	1.06
jd	0.712	73.07	74.36	−1.29	−15.7	0.95	1.09
ilm	0.237	63.83	63.41	0.42	—	1.20	1.34
sp	0.737	40.80	41.36	−0.56	−0.8	0.90	1.05
ru	0.379	31.43	32.63	−1.20	—	1.09	1.23
trid	0.037	17.37	17.45	−0.08	1.0	0.78	0.89
mang	0.229	31.59	33.41	−1.82	—	1.05	1.45
lime	0.161	21.34	21.94	−0.60	−1.5	0.91	1.01
per	0.071	15.70	15.75	−0.05	4.2	1.02	1.18
cor	0.176	25.35	22.60	2.75	8.5	0.91	1.08
herc	0.159	52.14	53.37	−1.23	11.2	1.00	1.13
hed	0.137	92.92	93.05	−0.13	−6.5	0.91	1.04
fs	0.313	96.54	96.45	0.09	−2.0	1.01	1.15
ky	0.353	38.21	40.04	−1.83	−3.0	0.85	1.01
sill	0.230	45.76	43.19	2.57	−0.9	0.84	0.98
caol	0.400	61.39	61.34	0.05	−6.7	0.83	0.93
larn	0.379	76.00	72.19	3.81	3.0	0.99	1.12
geh	0.208	108.36	108.08	0.28	6.2	0.90	1.02
ak	0.409	116.67	115.41	1.26	−0.1	0.92	1.03
mont	0.123	56.62	55.14	1.48	2.9	0.87	0.99
sph	0.298	77.65	77.45	0.20	—	0.96	1.08
fa	0.294	77.94	79.00	−1.06	2.7	1.09	1.22
fo	0.346	50.45	48.94	1.51	5.7	0.92	1.06
crd	0.502	173.90	176.51	−2.61	16.9	0.74	0.85
teph	0.621	84.80	84.28	0.52	—	1.10	1.22
wo	0.170	41.76	39.39	2.37	−0.8	0.84	0.95
cats	0.154	71.74	70.56	1.18	−3.5	0.91	1.05
di	0.234	76.51	78.02	−1.51	−8.0	0.91	1.04
en	0.533	69.86	71.71	−1.85	1.2	0.91	1.05
rho	0.160	52.44	50.86	1.58	—	1.01	1.14
tr	0.417	276.40	280.52	−4.12	−21.0	0.86	0.99
an	0.259	98.51	98.15	0.36	0	0.82	0.94
merw	0.478	154.60	153.75	0.85	−1.0	1.04	1.16
micr	0.632	105.48	106.57	−1.09	−0.8	0.81	0.91
kal	0.425	73.37	71.67	1.70	4.0	0.89	0.99
lc	0.315	95.93	93.32	2.61	12.1	0.84	0.94
ab	0.481	107.36	106.53	0.83	0	0.86	0.97
ne	0.323	70.19	71.64	−1.45	2.7	0.93	1.04
mu	0.530	146.87	149.08	−2.21	1.4	0.87	1.00
phl	0.394	166.30	165.45	0.85	4.4	0.88	1.01
ta	0.189	124.54	124.48	0.06	−7.9	0.83	0.97
pph	0.348	111.79	108.11	3.68	−3.4	0.82	0.96
anth	0.533	271.60	267.90	3.70	5.8	0.87	1.01
clin	0.879	186.70	186.58	0.12	−14.2	0.85	0.99
ma	0.240	134.00	136.46	−2.46	−0.8	0.88	1.03
pa	0.350	145.00	144.84	0.16	2.4	0.90	1.04
dia	0.039	17.55	19.15	−1.60	−0.3	0.95	1.15
gib	0.258	36.48	34.87	1.61	3.9	0.99	1.18
pre	0.304	152.50	154.27	−1.77	−2.8	0.89	1.02
chy	0.551	113.80	113.57	0.23	9.5	0.90	1.05
zo	0.377	160.00	158.70	1.30	4.9	0.93	1.07
alm	—	184.45	184.45	0	10.5	1.09	1.24
py	—	153.12	153.12	0	−13.7	1.01	1.16
gr	—	129.35	128.53	0.82	42.9	0.88	1.02
andr	—	154.56	156.17	−1.61	—	0.92	1.05

Note: Columns $(S - V)_{meas}$ and $(S - V)_{calc}$ are measured and calculated $S - V$; resid. is the residual in calculated entropy; RH is the equivalent residual calculated from the tables of Robinson and Haas (1983); k_D and k_E are the entropy/volume proportionality constants, defined in the text, for the Debye and Einstein theories; hat is the diagonal term from the hat (least-squares projection) matrix (Belsley et al., 1980) and indicates the influence of each observation on the least-squares solution, with hat = 0 denoting no influence and hat = 1 denoting extreme influence (forcing the fit through that datum).

* Abbreviations are given in Table 1.

ferent coordination states: The Fyfe et al. expression is recalled as

$$S_j = \Sigma n_i S_i + k(V_j - \Sigma n_i V_i),$$

where S_i and V_i are entropies and volumes of oxide components i, present in amount n_i, and S_j and V_j are the entropy and volume of the phase j. A certain amount of experience with measured data has shown that the value of k is approximately 1.0 if the units of entropy are in $J \cdot K^{-1} \cdot mol^{-1}$ and volumes are in $cm^3 \cdot mol^{-1}$. A petrological consequence of this is that solid-solid reactions involving no change in coordination state should have $dP/dT = \Delta S/\Delta V$ of approximately 10 $bar \cdot K^{-1}$. An example of such a reaction might be tremolite $\rightleftharpoons$ 2 diopside + talc. Unpublished experiments (Jenkins and Holland, in prep.) are in good agreement with this estimate, which should be reasonable for reactions, such as the one above, that involve little or no change in coordination. In contrast, reactions such as jadeite + quartz $\rightleftharpoons$ albite are driven by larger entropies, in part due to the increase in coordination state of Na and the change from octahedral to tetrahedral coordination of Al, and have somewhat larger dP/dT slopes (around 20 $bars \cdot K^{-1}$).

The method used here involves rearrangement of the above equation to the form

$$S_j = kV_j + \Sigma n_i(S_i - kV_i),$$

where the second term on the right is a constant for each oxide component. The values of the $(S_i - kV_i)$ and k were determined by least squares from measured entropies of oxides and silicates, with multiple regression returning $k = 1.00$ within error, in pleasing agreement with the simple harmonic oscillator model. Thus we may drop the constant k and fit the simpler model, taking S_i' to represent $(S_i - V_i)$,

$$S_j = V_j + \Sigma n_i S_i' \qquad (1)$$

to the experimentally measured entropies in Table 1 by regression. The resulting standard deviation of the residuals was 1.77 $J \cdot K^{-1} \cdot mol^{-1}$, and the average absolute deviation was 1.41 $J \cdot K^{-1} \cdot mol^{-1}$, with the worst deviation being 4.1 $J \cdot K^{-1} \cdot mol^{-1}$ (for tremolite). Table 2 shows the calculated results and the residuals in entropies for the phases used, and Table 3 lists the values for the entropies associated with each oxide component and their uncertainties (1σ).

The assignment of the components chosen requires brief comment. The 6-fold coordination of cations in the oxides Al_2O_3, MgO, CaO, FeO, TiO_2, and MnO are straightforward as are tetrahedral coordination for SiO_2, Al_2O_3, and MgO. In addition it was necessary to consider $^{[7]}$MgO to represent the slightly larger M2 site in orthopyroxenes and the M4 site in orthoamphiboles. Similarly, $^{[8]}$CaO refers to M2 clinopyroxene and M4 amphibole sites as well as the Ca in larnite and sphene. $^{[8-10]}$CaO represents Ca in much enlarged sites (e.g., in margarite) and/or those difficult to define precisely in terms of coordination num-

ber. K_2O was partitioned into $^{[a]}K_2O$ framework sites such as in feldspars and feldspathoids, and $^{[b]}K_2O$ sites such as in interlayer mica positions (and the large cavity of leucite); thus size and degree of vibrational freedom seem to categorize K_2O differences. Na_2O is partitioned into small $^{[8]}Na_2O$ as in pyroxene (M2) and amphibole (M4) sites and large $^{[9-12]}Na_2O$ as in framework silicates and micas. H_2O was the most difficult parameter to define; in the end, it was decided to split H_2O up into only two categories for simplicity. Although the nature of the bonding of the proton in hydrous silicates is very variable, it was found convenient to split mineral structures into a high-entropy H_2O(a) and a low-entropy H_2O(b) group. The micas fall naturally into high-entropy dioctahedral and low-entropy trioctahedral groups that may be rationalized on the basis of the distortion of the proton position in dioctahedral micas away from the normal to the mica sheets; in trioctahedral micas, the three full octahedral sites repel the proton equally (Bailey, 1984). In dioctahedral micas, the vacant M2 site causes the proton to be deflected largely into the vacant space, allowing for a greater degree of vibrational freedom. Chlorites are trioctahedral, with talc-like and brucite-like layers in which there is strong hydrogen bonding of the brucite hydroxyl groups to the talc layer oxygens, and so chlorites are attributed to the H_2O(b) group, as are talc, phlogopite, and the amphiboles. Diaspore, gibbsite, and serpentine are allocated to the H_2O(a) group because of the larger degree of freedom of the OH groups that are not strongly bonded to tetrahedral layers as in micas or, in the case of serpentines, because the layer mismatch between the octahedral and tetrahedral sheets allows more flexibility in the vibrational freedom of the hydroxyl groups.

It was also found that the large, 8-fold coordinated (distorted cube geometry), sites in garnet required separate evaluation; the entropy contribution from Ca in garnet $^{[gt]}$(CaO) is less than expected whereas the entropy contributions of iron $^{[gt]}$(FeO) and Mg $^{[gt]}$(MgO) are larger. For Mg, a small ion in a very large and somewhat distorted cage, the extra entropy is readily rationalized, but the low entropy for Ca seems anomalous.

To see the effect of ignoring the volume dependence of the entropy, a regression of the same data was performed without the volume terms, as done by Robinson and Haas (1983),

$$S_j = \Sigma n_i S_i, \qquad (2)$$

and the results are given in Table 3. The standard deviation of the residuals and the mean absolute deviation of the residuals were 3.26 and 2.50 $J \cdot K^{-1} \cdot mol^{-1}$, respectively, about twice the values of the volume-corrected model; however, the worst deviations were 9.85 $J \cdot K^{-1} \cdot mol^{-1}$ (larnite), 8.1 $J \cdot K^{-1} \cdot mol^{-1}$ (cordierite), and 7.5 $J \cdot K^{-1} \cdot mol^{-1}$ (leucite). Inspection of the results for Al_2O_3 reveals that with no volume correction, the difference between octahedral and tetrahedral coordination is 28.3 $J \cdot K^{-1} \cdot mol^{-1}$, whereas for the volume-corrected model, the difference is only 6.3 $J \cdot K^{-1} \cdot mol^{-1}$. The volume-independent model also fits the measured entropies rather better than the data of Robinson and Haas (1983) and may be useful in estimating entropies of mineral end-members for which no reliable volume data are available.

TABLE 3. Values for use with the entropy models

Component	$S - V$	σ_{S-V}	S	σ_S
$^{[4]}SiO_2$	17.45	0.38	40.30	0.39
$^{[6]}Al_2O_3$	22.60	0.84	43.78	0.84
$^{[4]}Al_2O_3$	28.89	1.06	72.07	1.05
$^{[6]}MgO$	15.75	0.53	26.67	0.54
$^{[4]}MgO$	18.77	1.77	38.30	1.77
$^{[7]}MgO$	21.06	1.36	27.74	1.35
$^{[gt]}MgO$	26.06	0.88	33.87	0.88
$^{[6]}CaO$	21.94	0.80	39.59	0.80
$^{[8]}CaO$	27.37	0.84	38.73	0.81
$^{[8-10]}CaO$	34.37	0.70	48.25	0.71
$^{[gt]}CaO$	17.86	0.67	29.47	0.99
$^{[4-8]}FeO$	30.78	0.83	43.24	0.83
$^{[gt]}FeO$	36.50	0.67	44.96	0.68
$^{[6]}MnO$	33.41	1.20	46.28	1.20
$^{[6]}TiO_2$	32.63	1.54	51.94	1.54
$^{[6]}Fe_2O_3$	50.24	1.60	80.51	1.61
$^{[8]}Na_2O$	56.32	3.67	65.86	4.58
$^{[9-12]}Na_2O$	79.49	3.12	97.28	3.13
$^{[a]}K_2O$	79.55	3.53	114.35	3.77
$^{[b]}K_2O$	87.96	3.03	120.37	3.37
H_2O(a)	15.71	0.91	30.03	0.91
H_2O(b)	7.44	0.87	20.74	1.03

Note. The first two columns of data, $S - V$ and its uncertainty, refer to the entropy-volume model, Eq. 1 in the text; the last two columns, S and its uncertainty, refer to the simple additivity model with no volume correction, Eq. 2 in the text.

APPLICATIONS

One of the motivating reasons behind this study was the need to estimate the entropies for minerals in a more general project to derive a reliable thermodynamic data set for petrological calculations. In earlier works (Powell and Holland, 1985; Holland and Powell, 1985), a preliminary thermodynamic data set was generated and used to obtain more powerful methods of characterizing metamorphic conditions, particularly pressure (Powell and Holland, 1988). The project is now at an advanced stage, involving many more mineral end-members and phase-equilibrium constraints, and has required the estimation of entropies of several phases where they were not known. It is also useful to have reliable entropy estimates for minerals even if complex thermodynamic calculations are not required, for instance when determining approximate slopes of univariant reactions from the Clausius-Clapeyron equation. The entropies for a number of rock-forming mineral end-members of interest are presented (Table 4), using the methods outlined above. Because it appears that magnetic transitions in silicate minerals tend to occur at very low temperatures, the tabulated entropies include the ideal magnetic contributions. It should be reemphasized, however, that site–configurational entropy terms have been omitted, as the degree of order in most silicates is at present poorly constrained. It is left to the

TABLE 4. Predicted entropies for unmeasured mineral end-members

Phase	V ($cm^3 \cdot mol^{-1}$)	S ($J \cdot K^{-1} \cdot mol^{-1}$)	$\pm\sigma_S$ ($J \cdot K^{-1} \cdot mol^{-1}$)	
		Chain silicates		
Johannsenite	68.1	179	2	$CaMnSi_2O_6$
Mg-Tschermak's pyroxene	58.9	123	2	$MgAl(SiAl)O_6$
Tschermakite	265.3	531	4	$Ca_2Mg_3Al_2(Si_6Al_2)O_{22}(OH)_2$
Endenite	270.9	588	5	$NaCa_2Mg_5(Si_7Al)O_{22}(OH)_2$
Pargasite	272.4	582	4	$NaCa_2Mg_4Al(Si_6Al_2)O_{22}(OH)_2$
Cummingtonite	264.7	533	5	$Mg_7Si_8O_{22}(OH)_2$
Grunerite	278.0	734	7	$Fe_7Si_8O_{22}(OH)_2$
Ferropargasite	279.4	703	5	$NaCa_2Fe_4Al(Si_6Al_2)O_{22}(OH)_2$
Ferroactinolite	282.8	705	6	$Ca_2Fe_5Si_8O_{22}(OH)_2$
Glaucophane	260.5	534	5	$Na_2Mg_3Al_2Si_8O_{22}(OH)_2$
Ferroglaucophane	265.8	624	6	$Na_2Fe_3Al_2Si_8O_{22}(OH)_2$
Riebeckite	274.9	691	6	$Na_2Fe_3Fe_2Si_8O_{22}(OH)_2$
Magnesioiriebeckite	271.3	602	6	$Na_2Mg_3Fe_2Si_8O_{22}(OH)_2$
		Sheet silicates		
Mg-celadonite*	139.7	288	2	$KMgAl(Si_4)O_{20}(OH)_2$
Eastonite	147.5	306	2	$KMg_2Al(Si_2Al_2)O_{20}(OH)_2$
Annite	154.3	405	3	$KFe_3(Si_3Al)O_{20}(OH)_2$
Siderophyllite	150.5	365	3	$KFe_2Al(Si_2Al_2)O_{20}(OH)_2$
Manganophyllite	157.9	421	4	$KMn_3(Si_3Al)O_{20}(OH)_2$
Na-phlogopite*	144.5	306	3	$NaMg_3(Si_3Al)O_{20}(OH)_2$
Amesite	209.2	388	4	$Mg_4Al_2(Al_2Si_2)O_{10}(OH)_8$
Daphnite	213.4	542	6	$Fe_5Al(AlSi_3)O_{10}(OH)_8$
Mn-clinochlore*	219.0	568	7	$Mn_5Al(AlSi_3)O_{10}(OH)_8$
Tschermak's talc*	132.9	250	2	$Mg_2Al(Si_3Al)O_{10}(OH)_2$
Minnesotaite	147.9	358	3	$Fe_3(Si_4)O_{10}(OH)_2$
Mn-talc*	150.5	373	3	$Mn_3(Si_4)O_{10}(OH)_2$
Mg-chloritoid*	68.8	132	2	$MgAl_2SiO_5(OH)_2$
Fe-chloritoid*	69.8	162	2	$FeAl_2SiO_5(OH)_2$
Mn-chloritoid*	71.0	167	2	$MnAl_2SiO_5(OH)_2$
		Others		
Mg-staurolite*	442.6	885	11	$Mg_4Al_{18}Si_{7.5}O_{48}H_4$
Fe-staurolite*	448.8	993	9	$Fe_4Al_{18}Si_{7.5}O_{48}H_4$
Mn-staurolite*	452.2	1013	10	$Mn_4Al_{18}Si_{7.5}O_{48}H_4$
Mg-carpholite*	105.9	194	2	$MgAl_2Si_2O_6(OH)_4$
Fe-carpholite*	106.9	223	2	$FeAl_2Si_2O_6(OH)_4$
Mn-carpholite*	108.2	229	2	$MnAl_2Si_2O_6(OH)_4$
Sapphirine	395.7	790	7	$Mg_6(MgAl)Al_6(Al_3Si_3)O_{40}$
Mg-pumpellyite*	295.5	629	6	$Ca_4Al_5MgSi_6O_{21}(OH)_7$
Vesuvianite	852.0	2008	16	$Ca_{19}Mg_2Al_{11}Si_{18}O_{69}(OH)_9$
Fe-cordierite*	237.1	470	3	$Fe_2Al_4Si_5O_{18}$
Mn-cordierite*	241.2	483	4	$Mn_2Al_4Si_5O_{18}$
Deerite	559.5	1531	13	$Fe^{2+}_{12}Fe^{3+}_{6}Si_{12}O_{40}(OH)_{10}$

Note: Entropies calculated from the entropy-volume model with no provision for Mg-Al or Si-Al disorder; however, the ideal magnetic entropy contribution has been added, on the assumption that transition metal–bearing silicates undergo low-temperature magnetic transitions.

* Names with elemental prefixes are not valid mineral names but represent idealized end-member (standard state) compositions in thermodynamic calculations.

user's judgement (or prejudice!) to add an appropriate entropy for disorder.

As a worked example, an estimation is made of the entropy of carpholite, $MnAl_2Si_2O_6(OH)_4$, for which the volume is 108.2 $cm^3 \cdot mol^{-1}$. All the Al is in octahedral coordination, and it is assumed that the H_2O is normal, i.e., like the trioctahedral micas. Thus, from Table 3, and Equation (1),

$$\begin{aligned} S_{\text{carpholite}} &= V_{\text{carpholite}} + (S - V)_{\text{MnO}} + (S - V)^{[6]}_{\text{Al}_2\text{O}_3} \\ &\quad + 2(S - V)_{\text{SiO}_2} + 2(S - V)_{\text{H}_2\text{O(b)}} \\ &= 108.9 + 33.41 + 22.60 + 2(17.45) \\ &\quad + 2(7.44) \\ &= 214.7 + \text{magnetic term.} \end{aligned}$$

Finally, one must add the ideal magnetic contribution for Mn^{2+}, of R ln 6, to yield $S = 229 \pm 2$ $J \cdot K^{-1} \cdot mol^{-1}$, the value given in Table 4.

CONCLUSIONS

The old concept of additivity of oxide components with a volume correction to yield estimates of mineral entropies is a useful one and has been improved upon by consideration of variable coordination states of cations in mineral structures. The proportionality constant in the entropy expression to allow for the volume effect has been found to be 1.0 if units of J, K, cm^3, and mol are used, and this value is in excellent agreement with predictions from the behavior of simple Einstein and Debye solids.

The entropies of silicate and multiple oxide phases may be estimated with uncertainties of about ± 2 to ± 3 $J \cdot K^{-1} \cdot mol^{-1}$ for most materials, but with slightly larger uncertainties (± 3 to ± 6 $J \cdot K^{-1} \cdot mol^{-1}$) for phases containing transition-metal ions. These uncertainties are lower than for any other simple method of estimation and in

many cases are not much larger than the experimental uncertainties themselves. In conclusion, molar volume should be viewed as a reliable monitor of the average bonding and vibrational state of minerals, a quality that makes molar volume useful in estimating entropies.

Acknowledgments

The helpful comments of Roger Powell at an early stage of this project are much appreciated, as are reviews by Bob Newton and Sue Kieffer that led to improvements in the discussion.

References cited

Anovitz, L.M., Treiman, A.H., Essene, E.J., Hemingway, B.S., Westrum, E.F., Wall, V.J., Burriel, R., and Bohlen, S.R. (1985) The heat capacity of ilmenite and phase equilibrium in the system Fe-Ti-O. Geochimica et Cosmochimica Acta, 49, 2027–2040.

Bailey, S.W. (1984) Crystal chemistry of the true micas. Mineralogical Society of America Reviews in Mineralogy, 13, 13–60.

Belsley, D.A., Kuh, E., and Welsh, R.E. (1980) Regression diagnostics: Identifying influential data and sources of collinearity. Wiley, New York.

Berman, R.G., and Brown, T.H. (1985) The heat capacity of minerals in the system K_2O-Na_2O-CaO-MgO-FeO-Fe_2O_3-Al_2O_3-SiO_2-TiO_2-H_2O-CO_2: Representation, estimation, and high temperature extrapolation. Contributions to Mineralogy and Petrology, 89, 168–183.

Bohlen, S.R., Metz, G.W., Essene, E.J., Anovitz, L.M., Westrum, E.F., and Wall, V.J. (1983) Thermodynamics and phase equilibrium of ferrosilite as a potential oxygen barometer in mantle rocks. EOS, 64, 350.

Bohlen, S.R., Dollase, W.A., and Wall, V.J. (1986) Calibration and applications of spinel equilibria in the system FeO-Al_2O_3-SiO_2. Journal of Petrology, 27, 1143–1156.

Carpenter, M.A. (1988) Thermochemistry of aluminium/silicon ordering in feldspar minerals. In E. Salje, Ed., Physical properties and thermodynamic behaviour of minerals. NATO ASI series C, 225, 265–323.

Fyfe, W.S., Turner, F.J., and Verhoogen, J. (1958) Metamorphic reactions and metamorphic facies. Geological Society of America Memoir 73, 259 p.

Haselton, H.T., and Westrum, E.F. (1980) Low temperature heat capacities of synthetic pyrope, grossular, and $pyrope_{60}grossular_{40}$. Geochimica et Cosmochimica Acta, 44, 701–709.

Haselton, H.T., Hemingway, B.S., and Robie, R.A. (1984) Low temperature heat capacities of $CaAl_2SiO_6$ glass and pyroxene and thermal expansion of $CaAl_2SiO_6$ pyroxene. American Mineralogist, 69, 481–489.

Haselton, H.T., Robie, R.A., and Hemingway, B.S. (1987) Heat capacities of synthetic hedenbergite, ferrobustamite, and $CaFeSi_2O_6$ glass. Geochimica et Cosmochimica Acta, 51, 2211–2217.

Helgeson, H.C., Delany, J.M., Nesbitt, H.W., and Bird, D.K. (1978) Summary and critique of the thermodynamic properties of rock-forming minerals. American Journal of Science, 278A, 229 p.

Henderson, C.E., Essene, E.J., Anovitz, L.M., Westrum, E.F., Hemingway, B.S., and Bowman, J.R. (1983) Thermodynamics and phase equilibria of clinochlore, $(Mg_5Al)(Si_3Al)O_{10}(OH)_8$. EOS, 64, 466.

Herrero, C.P., Gregorkiewitz, M., Sanz, J., and Serratosa, J.M. (1987) 29Si MAS-NMR spectroscopy of mica-type silicates: Observed and predicted distribution of tetrahedral Al-Si. Physics and Chemistry of Minerals, 15, 84–90.

Holland, T.J.B., and Powell, R. (1985) An internally consistent thermodynamic dataset with uncertainties and correlations: 2. Data and results. Journal of Metamorphic Geology, 3, 343–370.

Holland, T.J.B., and Richardson, S.W. (1979) Amphibole zonation in metabasites as a guide to the evolution of metamorphic conditions. Contributions to Mineralogy and Petrology, 70, 143–148.

Kieffer, S.W. (1980) Thermodynamics and lattice vibrations of minerals. 4. Applications to chain, sheet, and orthosilicates. Reviews in Geophysics and Space Physics, 18, 862–886.

——— (1982) Thermodynamics and lattice vibrations of minerals. 5. Applications to phase equilibria, isotope fractionation, and high pressure thermodynamic properties. Reviews in Geophysics and Space Physics, 20, 827–849.

Ko, H.C., Ferrante, M.J., and Stuve, J.M. (1977) Thermophysical properties of acmite. Proceedings of the 7th Symposium on Thermophysical Properties, American Society of Mechanical Engineers, 392–395.

Krupka, K.M., Robie, R.A., Hemingway, B.S., Kerrick, D.M., and Ito, J. (1985) Low temperature heat capacities and derived thermodynamic properties of anthophyllite, diopside, enstatite, bronzite, and wollastonite. American Mineralogist, 70, 249–260.

Latimer, W.M. (1951) Method of estimating the entropy of solid compounds. Journal of the American Chemical Society, 73, 1480–1482.

——— (1952) The oxidation states of the elements and their potentials in aqueous solutions, 392 p. Prentice-Hall, Englewood Cliffs, New Jersey.

Perkins, D., III, Essene, E.J., Westrum, E.J., and Wall, V.J. (1977) Application of new thermodynamic data to grossular phase relations. Contributions to Mineralogy and Petrology, 64, 137–147.

Perkins, D., III, Westrum, E.F., and Essene, E.J. (1980) The thermodynamic properties and phase relations of some minerals in the system CaO-Al_2O_3-SiO_2-H_2O. Geochimica et Cosmochimica Acta, 44, 61–84.

Powell, R., and Holland, T.J.B. (1985) An internally consistent thermodynamic dataset with uncertainties and correlations: 1. Methods and a worked example. Journal of Metamorphic Geology, 3, 327–342.

——— (1988) An internally consistent thermodynamic dataset with uncertainties and correlations: 3. Applications to geobarometry, worked examples and a computer program. Journal of Metamorphic Geology, 6, 173–204.

Price, G.D., Parker, S.C., and Leslie, M. (1987) The lattice dynamics and thermodynamics of the Mg_2SiO_4 polymorphs. Physics and Chemistry of Minerals, 15, 181–190.

Robie, R.A., and Hemingway, B.S. (1984a) Entropies of kyanite, andalusite, and sillimanite: Additional constraints on the pressure and temperature of the Al_2SiO_5 triple point. American Mineralogist, 69, 298–306.

——— (1984b) Heat capacities and entropies of phlogopite $(KMg_3[AlSi_3O_{10}](OH)_2)$ and paragonite $(NaAl_2[AlSi_3O_{10}](OH)_2)$ between 5 and 900 K and estimates of the enthalpies and Gibbs free energies of formation. American Mineralogist, 69, 858–868.

Robie, R.A., Hemingway, B.S., and Fisher, J.R. (1979) Thermodynamic properties of minerals and related substances at 298.15 K and 1 bar (10^5 Pascals) pressure and at higher temperatures. United States Geological Survey Bulletin 1452, 456 p.

Robie, R.A., Finch, C.B., and Hemingway, B.S. (1982a) Heat capacity and entropy of fayalite ($FeSiO_4$) between 5.1 and 383 K: Comparison of calorimetric and equilibrium values for the QFM buffer reaction. American Mineralogist, 67, 463–469.

Robie, R.A., Hemingway, B.S., and Takei, H. (1982b) Heat capacities and entropies of Mg_2SiO_4, Mn_2SiO_4, and Ca_2SiO_4 between 5 and 380 K. American Mineralogist, 67, 470–482.

Robie, R.A., Zhao, B., Hemingway, B.S., and Barton, M.S. (1987) Heat capacity and thermodynamic properties of andradite garnet, $Ca_3Fe_2Si_3O_{12}$, between 10 and 1000 K and revised values for $\Delta_f G^0$ (298.15 K) of hedenbergite and wollastonite. Geochimica et Cosmochimica Acta, 51, 2219–2224.

Robinson, G.R., and Haas, J.L. (1983) Heat capacity, relative enthalpy, and calorimetric entropy of silicate minerals: An empirical method of prediction. American Mineralogist, 68, 541–553.

Salje, E., and Werneke, Ch. (1982) How to determine phase stabilities from lattice vibrations. In W. Schreyer, Ed., High pressure researches in geoscience, E. Schweizerbart'sche Verlagsbuchhandlung, Stuttgart.

Sharp, Z.D., Essene, E.J., Anovitz, L.M., Metz, G.W., Westrum, E.F., Hemingway, B.S., and Valley, J.W. (1986) The heat capacity of a natural monticellite and phase equilibria in the system CaO-MgO-SiO_2-CO_2. Geochimica et Cosmochimica Acta, 50, 1475–1484.

Ulbrich, H.H., and Waldbaum, D.R. (1976) Structural and other contributions to the third law entropies of silicates. Geochimica et Cosmochimica Acta, 40, 1–24.

Wood, B.J. (1981) Crystal field electronic effects on the thermodynamic properties of Fe2+ minerals. In R.C. Newton, A. Navrotsky, and B.J. Wood, Ed., Thermodynamics of minerals and melts. Springer-Verlag, New York.

Manuscript received March 2, 1988
Manuscript accepted September 6, 1988